FAILURE ANALYSIS OF ULTRA-THIN CHOPPED CARBON FIBER TAPE REINFORCED THERMOPLASTIC IN DOUBLE-SHEAR TESTS

L. Meng*[1], I. Ohsawa[1] and J. Takahashi[1]

[1]Department of Systems Innovation, The University of Tokyo, Tokyo, Japan
*Email: meng-linshu@cfrtp.t.u-tokyo.ac.jp, Web Page: http://j-t.o.oo7.jp/index-e.html

Keywords: Chopped carbon fiber, Mechanical joints, Failure mechanism

ABSTRACT

Carbon fiber reinforced plastics (CFRP) nowadays are regarded as the potential substitution material for metallic structures in engineering to realize the weight reduction for engineering components. In the past years, carbon fiber reinforced thermosetting resins (CFRTS) has already been utilized in many industries such as aircraft and sports goods due to their outstanding specific modulus and strength. Compared with CFRTS, carbon fiber reinforced thermoplastics (CFRTP) own significant advantages such as short molding time, less hazardous chemical emission during manufacture processes and outstanding recyclability. Ultra-thin chopped carbon fiber tape reinforced thermoplastic (UT-CTT), as an emerging discontinuous CFRTP shows appealing potential for commercial applications as it bridges the gap between the lack of formability of continuous fiber composites and the lack of mechanical properties of short fiber composites. Excellent properties of UT-CTT showed promising prospect in the mass-production automobile to further promote the mitigation of the fossil consumption and slow down the problem of global warming. In this paper, an experimental study was carried out to investigate the failure characteristics of mechanical fastened UT-CTT. A parametric study considering the effects of geometric ratios, joining method and torque were conducted to identify the failure characteristics of mechanically fastened UT-CTT. Special failure modes that different with conventional composites materials were observed, and the joining method influenced the bearing strength a lot due to the suppression of tilt layer when the bolt exits. Besides, the bearing strength with small scatter, which offers positive signal to the realistic application of UT-CTT in the mass production of automobile.

1 INTRODUCTION

Carbon fiber reinforced plastic (CFRP) are divided into carbon fiber reinforced thermosetting resins (CFRTS) and carbon fiber reinforced thermoplastics (CFRTP) according to the difference of polymer used as matrix. CFRTS are expensive to produce but already widely used in the place where high strength-to-weight ratio and rigidity are required, such as aerospace, automotive, civil engineering, sports goods and an increasing number of other consumer and technical applications [1]. In contrast, CFRTP attracts more and more attention from researchers and engineers in recent years owing to the advantages of high recyclability, high secondary processing ability, short cycle time and cheaper price. Furthermore, seldom dangerous chemical emissions in manufacture process of CFRTP make the application of CFRTP becomes environmentally friendly in mass-production vehicles [2].

Unlike continuous CFRTP, discontinuous carbon fiber reinforced thermoplastic (DCFRTP) own excellent productivity and formability, but the poor mechanical property impeded the development and the application of DCFRTP. Recently, ultra-thin chopped carbon fiber tape reinforced thermoplastic (UT-CTT), a kind of randomly oriented strands (ROS) made by water dispersed thin tape, is a typical new material produced by compression molding with outstanding performance in both formability and mechanical properties. The UT-CTT material can fill the gap between continuous fiber composite with poor formability and discontinuous fiber composite with poor performance of mechanics [3]. Attractive mechanical performance and relatively low price leave UT-CTT promising prospects for mass production in automobile industry.

Among the most important elements in engineering composite structures in particular are mechanically fastened joints. Mechanically fastened joints own lots of overcoming advantages, such

as high strength, easy to disassembly to repair or replacement, the advantages make the mechanical fastening remains inescapable in automobile industry. Improper design of the joints may cause structural problems or conservative design, which will lead to overweight structures and high cost [4]. Thus, a large amount of attention has been paid to the study of mechanical joints to figure out the effects of numerous parameters on mechanical properties of joint structures, such as geometric parameters, joining method, clearance, pin-elasticity, clamping torque and washers etc. Due to the significance of this problem, mechanical fastened laminated composite plates have been studied by using analytical [5-6], numerical [7-8] and experimental methods [9-10] in the past years. Several approaches have been utilized to predict the bearing strength and failure modes of composite laminates in mechanical joints. However, little research about mechanical joint in chopped fiber tape material was conducted until now since it's an emerging material, whereas it is developing rapidly these years.

In this paper, the effects of geometric parameters on the bearing strength and failure modes in double-shear pin loaded and bolt loaded tests were investigated, the influence of torque in bolt loaded tests was also analysed and discussed.

2 PROCEDURE

2.1 Material

Ultra-thin chopped carbon fiber tape reinforced thermoplastic (UT-CTT) reveals excellent industrial development potential in automobile mass-production due to its outstanding mechanical property and acceptable price. UT-CTT is produced by compression molding with randomly oriented ultra-thin prepreg tapes, which are made up of carbon fiber (TR 50S, Mitsubishi Rayon Co., LTD.) and Polyamide-6 (PA6), the thickness of this tape is extremely thin (about 44 μm) compare with the conventional tape (150 μm). The thin-ply laminated composites can suppress the microcracking, delamination and splitting damage for static, fatigue and impact loadings, which draws a lot of attention in recent years [11].

Tapes are cut with 18 mm length and 5 mm width by digital cutter machine (G3M cutting machine, Zund, Swizerland) and Tomson cutter, after that through randomly dispersed and compression molding process, UT-CTT is shaped into the plate with the size of 250 mm × 250 mm. Afterwards, the plate are cut into specimens by using AC-500CF composite material cutting machine, the finished specimens have an average thickness of 3.3 mm with a fiber volume fraction (V_f) of 55%.

Tensile tests and compressive tests have been performed on UT-CTT rectangular specimens according to the ASTM D3039/D3039M-00 [12] and ASTM D3410/D3410M-03 [13] standards, parameters such as tensile modulus (E_t), compressive modulus (E_c) and Poisson's ratio (ν_{12}) etc. are determined as shown in Table 1.

	Symbol (Units)	Average	*CoV* (%)
Density	ρ (g/cm^3)	1.51	-
Tensile modulus	E_t (GPa)	40.8	3.43
Compressive modulus	E_c (GPa)	41.1	9.47
Poisson's ratio	ν_{12} (-)	0.28	10.3
Tensile strength	σ_t (MPa)	528	7.24
Compressive strength	σ_c (MPa)	370	3.39

Table 1: Properties of UT-CTT with 18 mm tape length.

2.2 Test configuration

The configuration of UT-CTT specimen is shown in Fig. 1(a), following the ASTM D5961/D5961M-13 standard [14], the length of all specimens are 100 mm, on the other hand, the width of the specimen and the distance from edge of specimen to the hole center were taken as geometric factors. In the pin loaded tensile tests, the specimens were 6 mm drilled to give 20 kinds of

specimens with *e/D*=1 to 5 and *w/D*=2 to 5. Additionally, 8 kinds of geometric ratios with *e/D*=1 to 5 when *w/D*=5, and *w/D*=2 to 5 when *e/D*=3 were conducted in the bolt loaded tensile tests. The specimens were tested in Shimadzu testing machine of 250 kN load capacity, and the double-lap fixture shown in Fig. 1(b) was used to perform the tests.

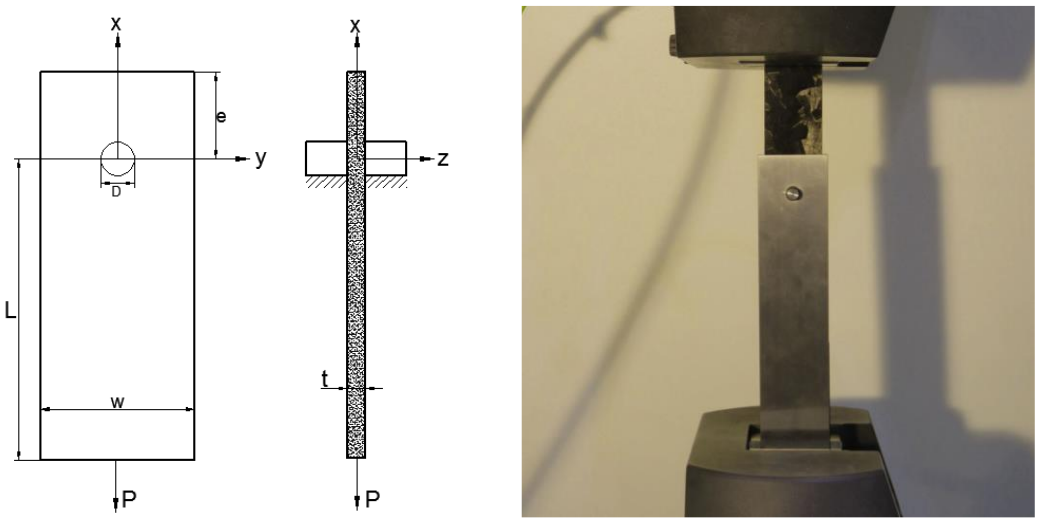

(a) (b)

Figure 1: Geometry of specimen with hole (a) and fixture assembly for double-lap joint (b).

Load is applied slowly with a speed of 0.4 mm/min when *w/D*=2 and 2 mm/min for other ratios, during the loading, the specimen is allowed to deform until it reaches ultimate failure, at which point the specimen cannot sustain any additional load. Following factors were observed during this process:

- Failure progression before ultimate failure.
- Failure modes.
- The load-displacement response for each specimen.
- The ultimate failure load.

Bearing strength is calculated with Eq. 1 [14] as following:

$$F^{bru} = P^{\max} / (k \times D \times t) \tag{1}$$

where F^{bru} is ultimate bearing strength, $P^{\max}$ is the maximum force prior to failure, k equals to 1 for single-fastener test, D is the diameter of the hole and t is the thickness of specimen.

3 RESULTS AND DISCUSSTION

3.1 Pin loaded tests

6 specimens were used when *e/D* and *w/D* ratios equal to 5, and 2 specimens were tested in other each ratio in pin loaded tests. 20 kinds of specimens with *e/D*=1 to 5 and *w/D*=2 to 5 were tested in Shimadzu testing machine of 250 kN load capacity.

3.1.1 Failure modes and bearing strength

Three types of failure modes were observed in the pin loaded double-shear tests as Table 2 shows. End fracture occurs when *e/D* ratio decrease to 1, fracture surface is shown as Fig. 2(a). In addition, abrupt failure of net section happens when *w/D* ratio is 2, shown as Fig. 2(b). When *w/D* and *e/D* ratio is big enough, which means *w/D* ratio is from 3 to 5 and *e/D* ratio is from 2 to 5, bearing failure occurs, shown as Fig. 2(c) and Fig. 2(d).

E: end fracture; N: net section; B: bearing

	e/D=1	*e/D*=2	*e/D*=3	*e/D*=4	*e/D*=5
w/D=2	E	N	N	N	N
w/D=3	E	B	B	B	B
w/D=4	E	B	B	B	B
w/D=5	E	B	B	B	B

Table 2: Failure modes under different *w/D* ratio and *e/D* ratio.

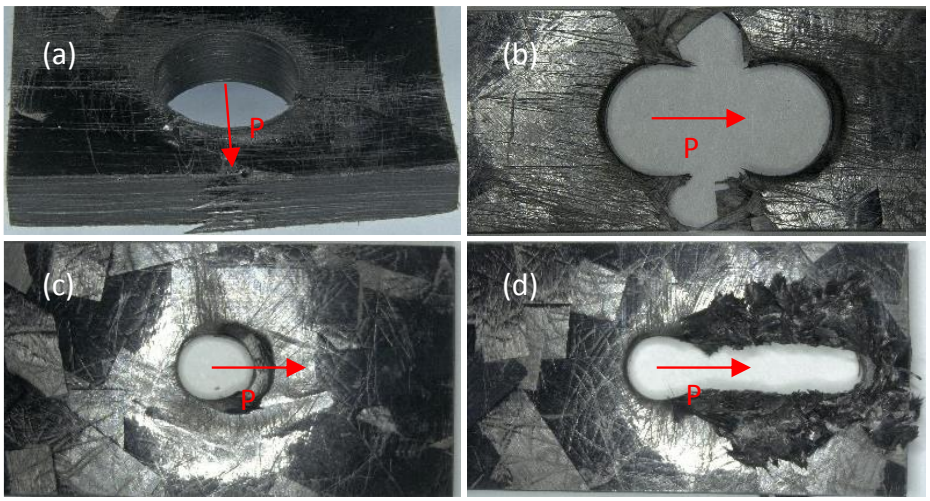

Figure 2: Appearance of failure modes in pin loaded tests. (a). End Fracture (b). Net section (c). Bearing failure (d). Progressive failure after bearing failure (P: Pin loading direction).

When *e/D* and *w/D* ratios equal to 5, the average bearing strength is approximate 473 MPa and *CoV* is only 2.18%, small *CoV* indicates the bearing strength are stable for different specimens, which shows promising potential in actual engineering application of UT-CTT material.

As shown in Fig. 3, bearing strength increases when *e/D* ratio increases from 1 to 2, at this time, the failure modes changes from end fracture failure to net section and bearing failure. After that, the bearing strength becomes almost stable with the increase of *e/D* ratio, which means an increase in edge distance does not seem to affect bearing strength under same failure mode. Similarly, bearing strength increases when *w/D* ratio increases from 2 to 3, and failure mode changes from net section to end fracture and bearing failure at this time. Moreover, the bearing strength is not affected by the increase of width under bearing failure mode when *w/D* ratio is from 3 to 5. The abnormal variation when *e/D* equals to 1 may be mainly caused by big scatter, because the tape length is 18 mm, but the distance from pin edge to specimen end is only 3 mm.

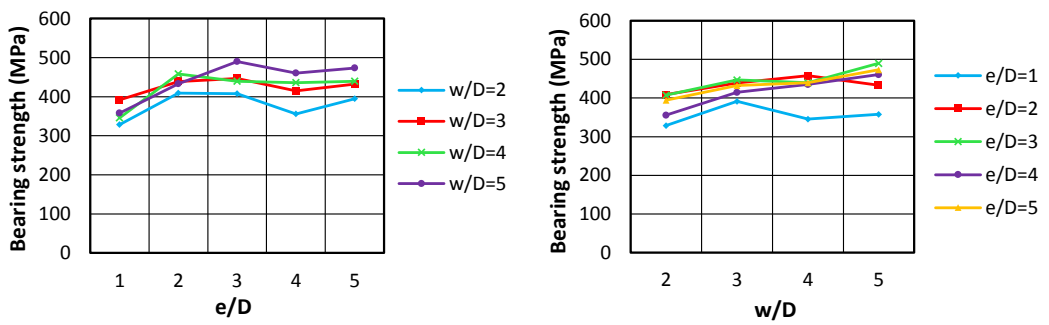

Figure 3: The effects of *e/D* (left) ratio and *w/D* (right) ratio on the pin loaded bearing strength.

3.1.2 Fractography

Several specimens with *w/D*=5 and *e/D*=5 were unloaded after loading to setting levels for fractography of bearing failure process, they were cut along the centerline of the specimen, afterwards observed by KEYENCE VHX-1000 digital microscope in detail as shown in Fig. 4. The load levels were defined as 50%, 75% and 100% of the maximum load, moreover, another specimen was overloaded to observe the failure details after maximum load.

We found that the main damage patterns are fiber compressive failures involving fiber buckling and lamina delamination. Failure cannot be observed at the load level of 50% of maximum load, when the load increases to the 75% of maximum load, delamination starts to occur, after that, distinct through-thickness buckling failure and delamination occurs at the peck point of the load curve (maximum load), the great range bucking squeeze the surface lamina tilt in thickness direction. After the peak, the buckling and delamination failure further developed mainly along the maximum shear stress direction (45˚) from center point to the surface, and the central part starts to be sinking.

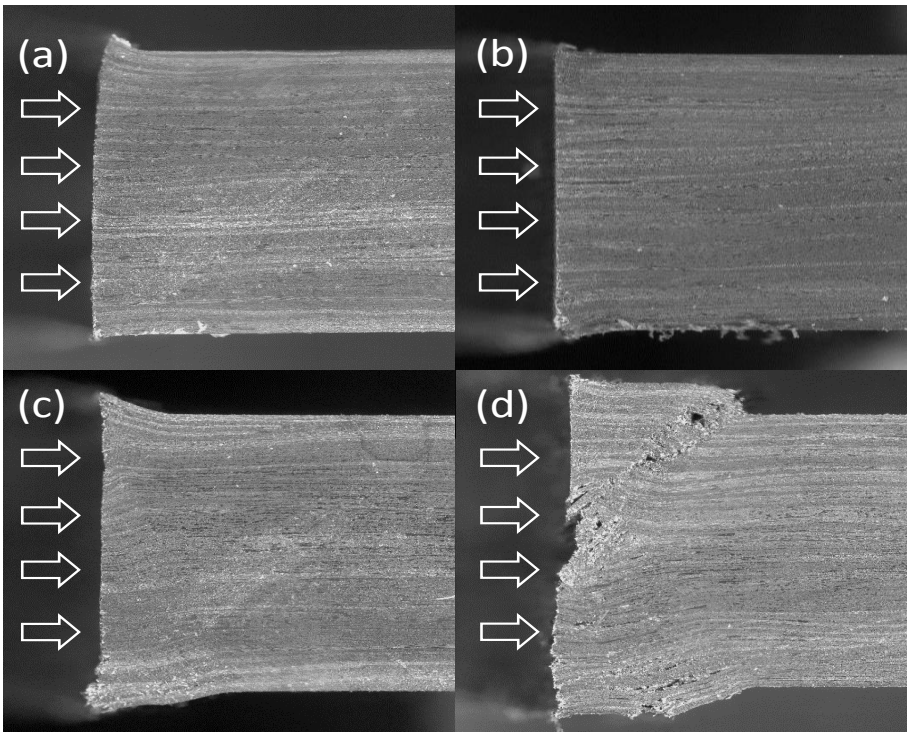

Figure 4: Photographs of through-thickness bearing damage. (a) 50% (b) 75% (c) 100% of maximum load, (d) after maximum load. (Arrow: pin load direction).

3.2 Bolt loaded tests

5 specimens were used when *e/D* and *w/D* ratios equal to 5 and 1 specimen was tested in other each ratio with different torques of 0 N·m, 3 N·m and 6 N·m in bolt loaded tests. 8 kinds of geometric ratios with *e/D*=1 to 5 when *w/D*=5 and *w/D*=2 to 5 when *e/D*=3 were conducted in Shimadzu testing machine of 250 kN load capacity.

3.2.1 Failure modes and bearing strength

Four types of failure modes were observed in the bolt loaded double-shear tests as Table 3 shows. End fracture occurs when *e/D* ratio decrease to 1, fracture surface is shown as Fig. 5(a). Cleavage happens when *e/D* ratio is 2, as the Fig. 5(b) shows. In addition, abrupt failure of net section happens when *w/D* ratio decreases to 3, shown as Fig. 5(c). When *w/D* and *e/D* ratio are big enough, which means *w/D* ratio is from 4 to 5 and *e/D* ratio is from 3 to 5, bearing failure occurs, shown as Fig. 5(d).

E: end fracture; C: cleavage; N: net section; B: bearing

	e/D=1	*e/D*=2	*e/D*=3	*e/D*=4	*e/D*=5
w/D=2			N		
w/D=3			N		
w/D=4			B		
w/D=5	E	C	B	B	B

Table. 3: Failure modes under different *w/D* ratio and *e/D* ratio.

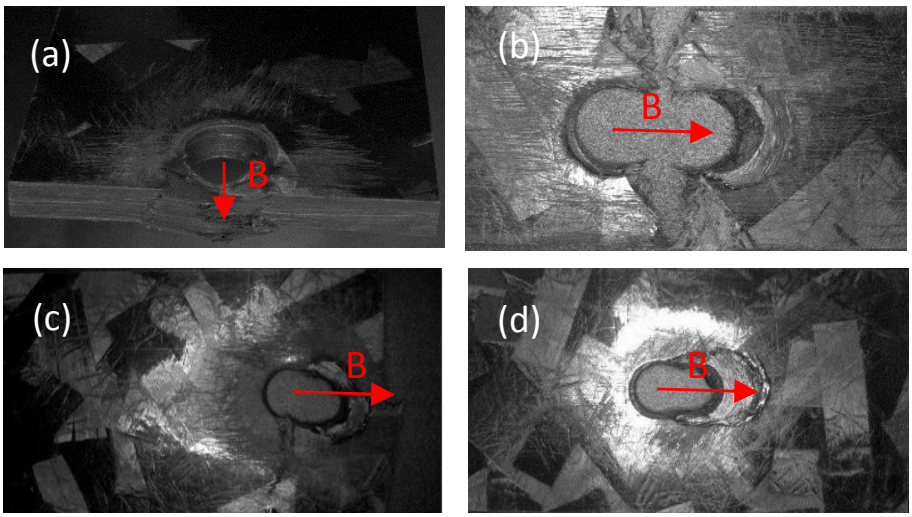

Figure 5: Appearance of failure modes in bolt loaded tests. (a). End Fracture (b). Net section (c). Cleavage (d). Bearing failure (B: Bolt loading direction).

The effects of *w/D* ratio and *e/D* ratio on the bearing strength of UT-CTT in bolt loaded tests are shown in Fig. 6. Bearing strength increases from 381 MPa to 769 MPa when *e/D* ratio increases from 1 to 2, and failure mode changes from end fracture to cleavage failure at this time. Afterwards, the bearing strength become stable with the increase of *e/D* ratio even the failure mode changes from cleavage to bearing failure when *e/D* ratio increases from 2 to 3, it shows that the bearing strength with cleavage failure when *e/D* is 2 is almost same with the bearing strength of bearing failure in bolt loaded tests.

Similarly, bearing strength increases from 318 MPa to 739 MPa when *w/D* ratio increases from 2 to 3, at this time, the failure modes are both net section failure. After that, the bearing strength become almost stable with the increase of *w/D* ratio even though the failure mode changes from net section to bearing failure when *w/D* ratio increases from 3 to 4, which means the bearing strength with net section failure when *w/D* is 3 is close to the bearing strength of bearing failure in bolt loaded tests.

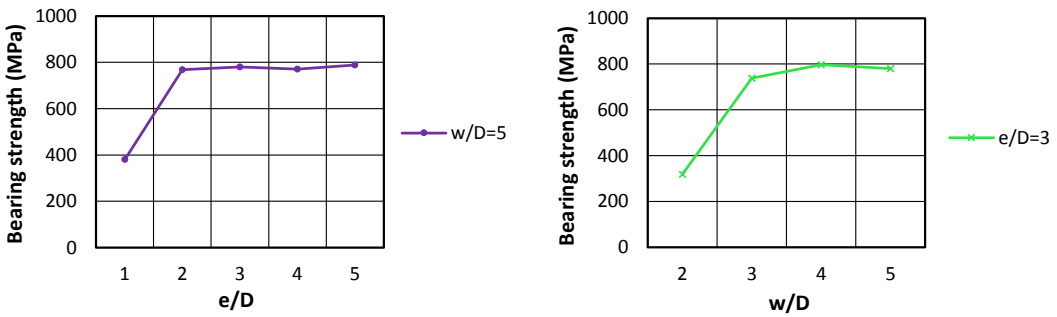

Figure 6: The effects of *e/D* ratio (left) and *w/D* ratio (right) on the bolt loaded bearing strength.

3.2.2 Effects of torque

In the tests with geometric ratios *w/D*=5 and *e/D*=5, as shown in Fig. 7, the bearing strength in bolt loaded tests are 771 MPa, 781 MPa and 781 MPa when the torques are 0 N·m, 3 N·m and 6 N·m separately, the *CoV* shows stable around 2% to 3% with different torques. In other words, the results show that the torque don't have obvious influence on the failure modes and bearing strength in different geometric ratios.

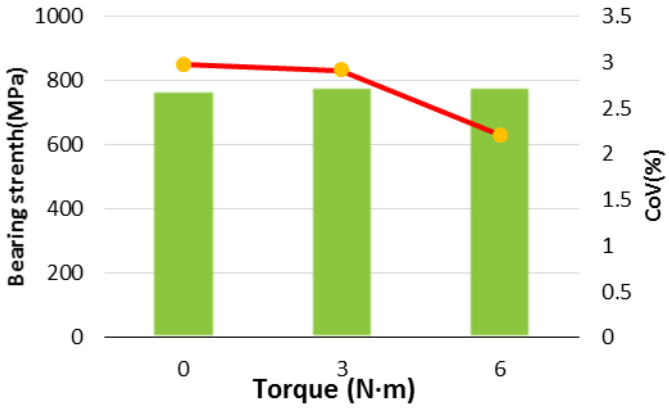

Figure 7: Bearing strength and *CoV* when *w/D*=5 and *e/D*=5 with different torques.

3.2.3 Fractography

Similar to previous section, two specimens with *w/D*=5 and *e/D*=5 under 0 N·m torque were unloaded after loading to two setting levels, the specimens were also cut along the centerline of the specimen to observe the inner damage details by using digital microscope.

The results of the two levels of failure photographs are shown as Fig. 8. These photographs also show that the main damage patterns are fiber compressive failures involving fiber buckling and lamina delamination. As we could see from Fig. 8(a), distinct through-thickness buckling failure and delamination occurs at this time, which is similar to Fig. 4(c) (the load are both around 9 kN) at the peck point of the load curve, however, because fixture loading plate could suppress further delamination of the tilt of surface layer when the bolt exits, which could make the specimen continue to sustain the increasing load. In addition, as Fig. 8(b) shows, until 100% of maximum load in bolted test, continuous zig-zag buckling occurs to sustain the increasing load, even after the peak, the buckling proceed with the increasing of the bolt displacement, and the load started to slowly decrease after the peak.

Owing to the suppression of delamination and the tilt of surface lamina could ensure the central part continue to sustain the load instead of becoming sunk comparing with Fig. 4(d), during the failure process, obvious tilt of the surface layer was suppressed due to the exit of bolt, the bolt was tightened up before it got to final failure. Thus, bolt with different torques produce same suppression effect on the specimen, then the specimens fail at almost same strength with different torques, which leads to the specimens also have same failure modes with different torques.

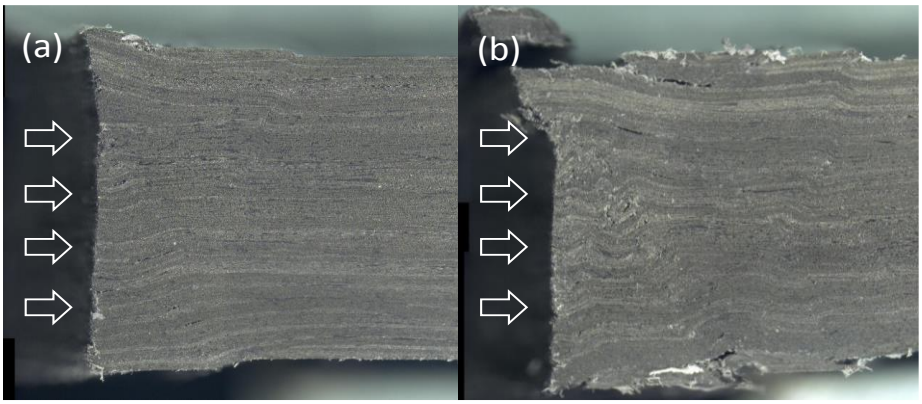

Figure 8: Photographs of through-thickness bearing damage. (a) 60% (b) 100% of maximum load. (Arrow: bolt load direction).

3.3 Comparison

For the specimens with *w/D*=5 and *e/D*=5, the pin and bolt loaded (0 N·m) tests are compared and the results are shown in Fig. 9, the average bearing strength in pin loaded tests is 473 MPa and the average bearing strength is 771 MPa in bolt loaded tests. Due to the suppression of delamination and surface layer tilt in bolt loaded tests, the bearing strength increase 63% when the loading method changes from pin to bolt. At this time, the *CoV* of bearing strength changes from 2.18% to 2.98%, the small *CoV* in both pin and bolt loaded tests bring out the practical significance for the application of UT-CTT in mass production automobile.

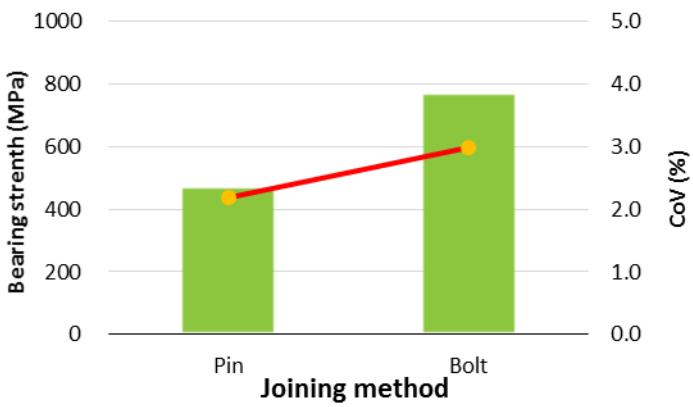

Figure 9: Bearing strength and *CoV* when *w/D*=5 and *e/D*=5 in different joining method.

4 CONCLUSIONS

In present research, pin and bolt loaded double-shear tests with 18mm tape length UT-CTT were performed. Effects of geometric factors on failure modes and bearing strength were investigated, afterwards, the effects of three kinds of different torques in bolted tests were also figured out. Finally, fractography was conducted to observe the failure details during the bearing failure process. The conclusions are given as below:

- The bearing strength increase 63% simply changing the loading method from pin to bolt, at this time, with regard to the critical ratios of failure modes converted to bearing failure, the critical *e/D* ratio changes from 2 to 3, and critical *w/D* ratio converted from 3 to 4 because of the increasing of maximum load due to the suppression effects when the bolt exit.
- Bearing strength almost does not be influenced by *e/D* and *w/D* ratio under same failure modes in both pin and bolt loaded tests. Besides, in the bolt loaded tests, the torque has no apparent effects

on the bearing strength.

- The *CoV* of bearing strength is 2.18% in the pin loaded tests, and the *CoV* changes from 2% to 3% with different torques in the bolt loaded tests. Both pin and bolt loaded tests with small value of *CoV* results, which shows promising potential in actual engineering application of UT-CTT material.
- In both pin and bolt loaded tests, fiber compressive failures involving fiber buckling and lamina delamination were observed as main damage patterns. However, because of the suppression of the fixture loading plate during the failure process in bolt loaded tests, continuous zig-zag buckling occurs and specimen could continue to sustain the increasing load, instead of severe delamination and layer tilt in through thickness direction in pin loaded tests.

ACKNOWLEDGEMENTS

Part of this study was conducted as Japanese METI project "the Future Pioneering Projects/Innovative Structural Materials Project" since 2013fy. Part of the work was assisted by Sanko Gosei Ltd and Industrial Technology Center of Fukui Prefecture. Authors would like to express sincerely appreciation to all of them.

REFERENCES

[1] D. Hull and T.W. Clyne, *An Introduction to Composite materials*, Cambridge solid state science series, Cambridge University Press, Cambridge, 1996.

[2] J. Takahashi and T. Ishikawa, Next challenge in CFRTP for mass production automotive application, *SEICO 14 SAMPE EUROPE 35th. International Conference and Forum, Paris, France,* 2014.

[3] M. Selezneva, S. Meldrum, S. Roy, et al., Modeling of Mechanical Properties of Randomly Oriented Strand Thermoplastic Composites, *The 16th European Conference on Composite Materials, Seville, Spain,* 2014.

[4] Y. Tang, Z. Zhou Z, S. Pan, J. Xiong J and Y.Guo, Mechanical property and failure mechanism of 3D Carbon–Carbon braided composites bolted joints under unidirectional tensile loading, *Materials & Design,* **65**, 2015, pp. 243-253.

[5] B. Okutan, The effects of geometric parameters on the failure strength for pin loaded multi-directional fiber-glass reinforced epoxy laminate, *Composites Part B: Engineering,* **33**, 2002, pp. 567-578.

[6] Z. Wang, S. Zhou, J. Zhang, X. Wu, L. Zhou, Progressive failure analysis of bolted single-lap composite joint based on extended finite element method, *Materials & Design,* **37**, pp. 582-588, 2012.

[7] C.C. Lin, C.H. Lin, Stresses around pin loaded hole in composite laminates using direct boundary element method, *International Journal of Solids and Structures,* **36**, 1999, pp. 763-783.

[8] A. Barut, E. Madenci, Analysis of bolted–bonded composite single-lap joints under combined in-plane and transverse loading, *Composite Structures,* **88**, 2009, pp. 579-594.

[9] J.C. Chen, C.K. Lu, C.H. Chiu, H. Chin, On the influence of weave structure on pin loaded strength of orthogonal 3D composites, *Composites,* **25**, 1994, pp. 251-262.

[10] C. Cooper, G.J. Turvey, Effects of joint geometry and bolt torque on the structural performance of single bolt tension joints in pultruded GRP sheet material, *Composite Structures,* **32**, 1995, pp. 217-226.

[11] S. Sihn, R.Y. Kim, K. Kawabe and S.W. Tsai, Experimental studies of thin-ply laminated composites, *Composites Science and Technology,* **67**, 2007, pp. 996-1008.

[12] ASTM D 3039/D 3039M-00, Standard Test Method for Tensile Properties of Polymer Matrix Composite Materials, *American Society for Testing of Materials,* 2002.

[13] ASTM D 3410/D 3410M-03, Standard test Method for Compressive Properties of Polymer Matrix Composite Materials, *American Society for Testing of Materials,* 2008.

[14] ASTM D5961/D5961M-13, Standard Test Method for Bearing Response of Polymer Matrix composite Laminates, *American Society for Testing of Materials,* 2013.